International Journal of Applied Science and Mathematics
Volume 2, Issue 5, ISSN (Online): 2394-2894

Synthesis of Mn^{2+} Ions Doped ZnS Nanoparticles using PVP, TOPO and CTAB as Capping Agent and their Characterization

R. Ashok Kumar, K. Geetha* and P. Prabukanthan
PG & Research Department of Chemistry,
Muthurangam Government Arts College, Vellore – 632 002.

Abstract **– Mn^{2+} ions doped ZnS nanoparticles were synthesized at 80^0C through a soft chemical route, by chemical co-precipitation method at open atmosphere. The water soluble PVP, TOPO and CTAB were used as capping agents of synthesis Mn^{2+} ions doped ZnS nanoparticles. The nanostructure of the synthesized Mn^{2+} ions doped ZnS nanoparticles were characterized by powder X-ray diffraction (XRD), Scanning election microscope (SEM), transmission electron microscope (TEM), Fourier transform infrared spectrometer (FT-IR), UV-vis spectra . The size of as prepared Mn^{2+} ions doped ZnS nanoparticles is found to be around 1.07-8 nm range. The room temperature photoluminescence (PL) spectra showed a broad blue emission band observed between 450-580nm.**

Keywords **– Mn^{2+} ions, ZnS, Nanoparticles, PVP, TOPO, CTAB, X-ray diffraction (XRD), Scanning Election Microscope (SEM), Photoluminescence (PL).**

I. INTRODUCTION

Nanocrystalline materials have been of interest for more than 20 years and this interest is still increasing [1-8]. The main cause is in their unusual properties based on the high concentration of atoms in interfacial structures and the relatively simple ways of their preparation. Nanoparticles of zinc- sulphide compounds prepared by precipitation techniques have been investigated very frequently with the aim to prepare homogeneous distribution of atoms in order to improve their electrical and optical properties [9-11]. Among the II–VI semiconductors ZnS is widely studied owing to its stability and technological application [12-13] ZnS nanoparticles doped with metallic elements has a variety of application [14] and also ZnS an important semiconductor compound of the II-VI group with excellent physical properties and wide band gap energy of 3.7 eV at 300 K has attracted great attention. It has been extensively investigated due to its potential device applications such as window layers for solar cells, optoelectronics, data storage devices, quantum dot laser, nano sensors, nano phosphors, biological markers and efficient photocatalysis [15-17]. Luminescent properties of ZnS can be controlled using various dopands such as Ni, Te, Mn, Cu etc. Nevertheless, II-VI semiconductor nanoparticles are themselves highly unstable and in the absence of a trapping medium or some other form of encapsulation they agglomerate or coalesce quickly [18]. If this growth of particles is not controlled, the particles agglomerate and settle due to Ostwald ripening and Vander Waals interaction between particles [19]. For the reason capping agent to the nanoparticles is necessary to provide surface passivation and also to improve the surface state, which significantly influence the optoelectronic properties of nanoparticles [20-21]. In general the agglomeration can be arrested by two factors first electro statically and second inducing steric, when a polymer is adsorbed on to a surface. In general does not lie flat rather some parts of the polymer are adsorbed on the surface while other portions of the chain extend away from the surface into the medium. When two such polymer layer overlaps at a collision distance between the particles repulsion occur. Thus a polymer can provide a strong repulsion between two approaching surfaces a small portion of the molecule must be tightly adsorbed to the underlying nanoparticles surface while most of the polymer chain should extend away from the surface. This paper reports a simple route for the preparation of undoped and Mn doped ZnS nanoparticles via the chemical precipitation method. The water soluble PVP, TOPO, CTAP were used as capping agents. The prepared nanoparticles were characterized. The grain size is calculated from the XRD line broadening and morphology of same sample was studied from TEM analysis. Capping molecules were identified by FT-IR. The impurity (Mn) was identified by ESR. The optical properties of the sample was studied by UV- Vis and photoluminescence. The thermal properties Were Studied by TG-DTA.

II. EXPERIMENTAL

The synthesis of pure and Mn dopped ZnS were carried out at room temperature and all chemicals used were of analytical grade. First, a desired molar proportion of $Zn(CH_3COO)_2.2H_2O$ in 50 ml deionized water and $Mn(CH_3COO)_24H_2O$ (wt% in Mn= 1 %, 2 %, 3 % and 4 %) in 50 ml deionized water were dissolved and surfactant was added to control the growth of the nano crystals during the reaction. Subsequently, the Na_2S (50ml) was added drop wise by an additional funnel to the above mixture. For each experiment, the molar amounts of $Zn(CH_3COO)_2$ and Na_2S used were equal. Undoped ZnS nanoparticles were synthesized by following the same procedure without doping and capping agents (PVP TOPO and CTAB). For the synthesis of surfactants capped ZnS:Mn^{2+} nanoparticles, the surfactant should be added. During the whole reaction process, the reactants were vigorously stirred under open atmosphere at 80˚ C. The formed nanocrystals were separated from the solution by centrifuging. After washing repeatedly with deionized water and then drying at 100˚C under vacuum, the powder

samples of ZnS:Mn^{2+} nano-particles were obtained. The X-ray diffraction (XRD) patterns of the powdered samples were recorded using X'PERT-PRO diffractometer with a CuKα radiation (λ 1.5406˚A) under the same conditions. The particle size was estimated using Scherer's equation (0.9 λ)/ (β cosθ) at full width at half maximum of the major XRD peak. The size and morphology of the nanoparticles were determined using TEM (PHILIPS-CM200; 20–200kV). For sample preparation, dilute drops of suspension were allowed to dry slowly on carbon-coated copper grids for TEM measurement. The FT-IR spectra were recorded on an AVATOR360 spectrometer. The optical transmission spectra of the same particles in de-ionized water were recorded using UV-1650PC the thermal analysis was carried out with SDTQ60020 thermometer.

PVP,TOPO and CTAB capped Zns:Mn^{2+} nanoparticles were synthesized by following a simple reaction in aqueous solution.

$Zn(C_2H_3O_2)_2 + Mn^{2+} (C_2H_3O_2)_2 + PVP/TOPO/CTAB \rightarrow PVP/TOPO/CTAB - (Zn + Mn^{2+}) + 4CH_3COO^- + 2Na_2S$

$PVP/TOPO/CTAB-(Zn+Mn^{2+}) + 4CH_3COO^- + 2Na_2S \rightarrow PVP/TOPO/CTAB- (ZnS:Mn) + 4Na (C_2H_3O_2)$

III. Result and Discussion

Structure and morphological studies

Fig. 1 Illustrates the XRD patterns of the pure ZnS and, Mn^{2+} doped ZnS and surfactants capped ZnS:Mn^{2+} nanoparticles. It shows very broad diffraction peaks, which are the characteristic of nano sized materials. For all the samples three diffraction peak positions correspond to the lattice planes of (111), (220) and (311), which matches very well with the cubic zinc blend structure.

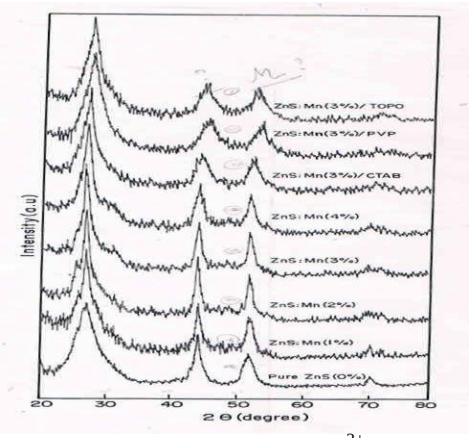

Fig.1. XRD spectra of ZnS, ZnS : Mn^{2+} (1% - 4%) and different surfactant (PVP, TOPO,CTAP) capped ZnS: Mn^{2+} nanoparticles

No diffraction peaks from manganese impurities were detected. Thus it is observed that the Mn^{2+} ions are dispersed into the ZnS matrix. According to the Debye–Scherer formula, the mean crystalline sizes calculated from the full- width at half-maximum (FWHM) of these lines are about 8.55 nm for uncapped ZnS and 5 nm for ZnS:Mn^{2+} nanoparticles. Further, relatively larger line broadening in surfactant (PVP, TOPO and CTAB) capped sample indicates their smaller particle size as compared to uncapped samples. From the XRD line width, they earn crystalline domain sizes which have been estimated to be around 1.072, 1.218 and 1.52 nm for PVP. TOPO and CTAB capped ZnS:Mn^{2+} particles, respectively.

This result indicates necessity of the capping agent for the reduction of particles size. By comparing the effect of three surfactant, the PVP is used as an effective surfactant reduce the particles size, which may be due to the presence of the strong dipole moment nitrogen-oxygen bond in this surfactant. A typical SEM micro photographs of ZnS and ZnS:Mn^{2+} nanoparticles (Fig.2a-b) show that the particles have smooth surface and an average agglomerate size of around 30 nm.

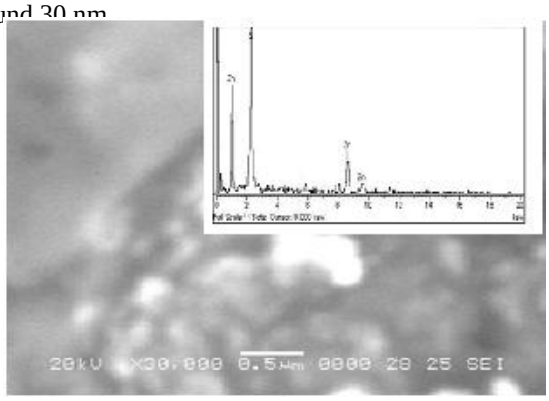

Fig.2. (a) SEM spectrum of Pure ZnS compound and EDAX spectrum

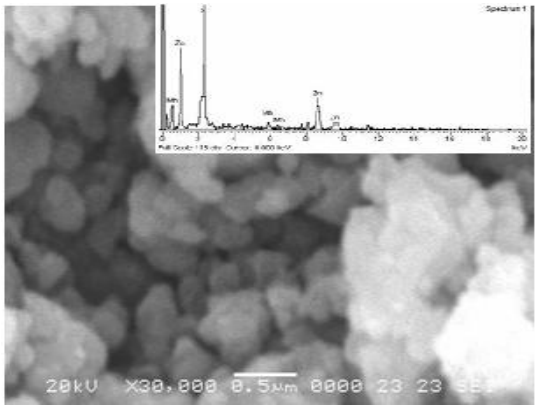

Fig.2. (b) SEM Spectrum of 1% MN^{2+} Doped ZnS compound and EDAX spectrum

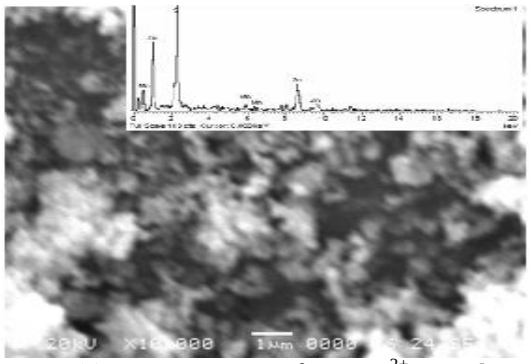

Fig.2. (c) SEM Spectrum of 2% Mn^{2+} Doped ZnS compound and EDAX

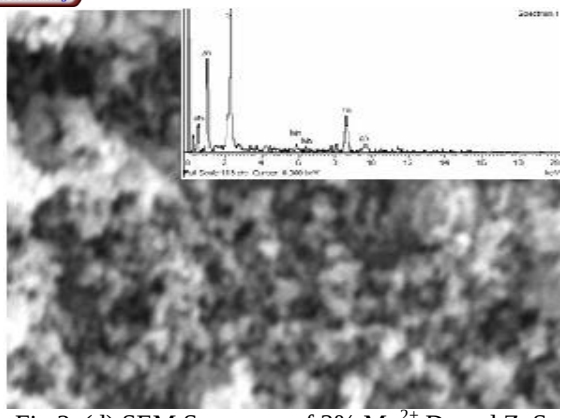

Fig.2. (d) SEM Spectrum of 3% Mn^{2+} Doped ZnS compound and EDAX spectrum.

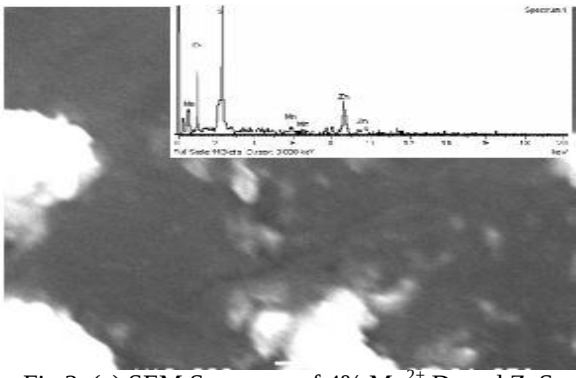

Fig.2. (e) SEM Spectrum of 4% Mn^{2+} Doped ZnS compound and EDAX spectrum.

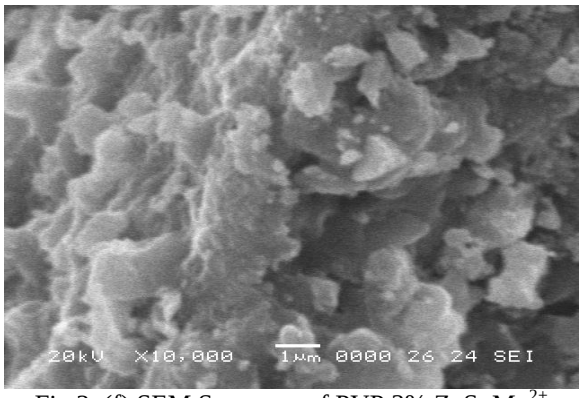

Fig.2. (f) SEM Spectrum of PVP 3% ZnS; Mn^{2+} nanoparticles EDAX spectrum.

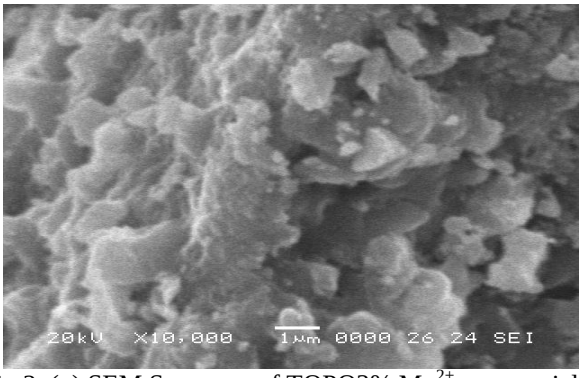

Fig.2. (g) SEM Spectrum of TOPO3% Mn^{2+} nanoparticles

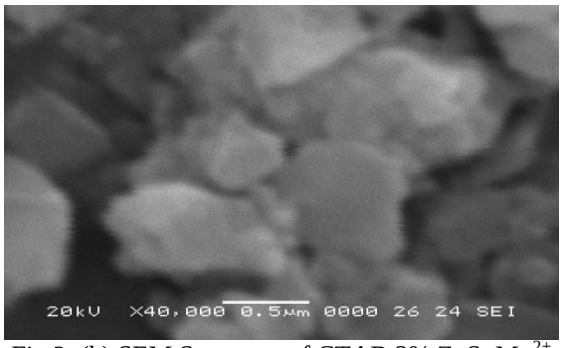

Fig.2. (h) SEM Spectrum of CTAB 3% ZnS; Mn^{2+} nanoparticles

But the actual size of the nanoparticles cannot be determined from the SEM images, as it is limited by the resolution of the used SEM instrument (The actual particle size calculated through XRD diffraction is 8.55 and 5 nm). The elemental composition determined through EDAX attached with SEM instrument is shown in Fig 2(a-b) for ZnS and ZnS:Mn^{2+} nanoparticles, respectively. This reveals that the Mn^{2+} ions are incorporated in the Zn^{2+} lattice sites. SEM image of different concentration of ZnS:Mn^{2+} nanoparticles (1%-4%) with corresponding elemental dispersive X-ray spectrum are shown the Fig 2 (a-e). The different surfactant capped PVP, TOPO and CTAB capped ZnS:Mn^{2+} nanoparticles were shown in the fig 2(f-h). Fig.3 TEM image of PVP capped ZnS:Mn^{2+} nanoparticles. Fig.3(a-e,) shows TEM images of the pure ZnS, ZnS; Mn^{2+},PVP, TOPO and CTAB capped ZnS:Mn^{2+} (3%) nanoparticles, respectively. The TEM images indicate, the synthesized particles are spherical in shape and homogeneous distribution. The TEM images of PVP capped particles reveal the distinct grain boundaries (Fig. 3c) with an average crystallite size about 8.5 nm and 5 nm for capped ZnS:Mn^{2+} nanoparticles.

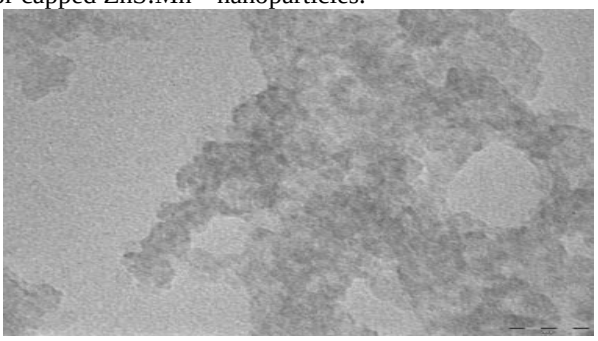

Fig.3. (a) TEM image of the pure ZnS compound

Fig.3. (b) TEM image of the ZnS:Mn^{2+} nanoparticles

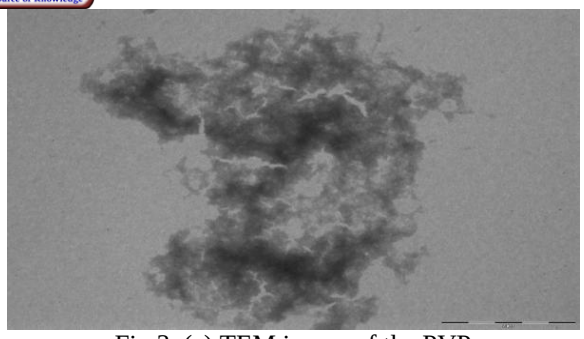

Fig.3. (c) TEM image of the PVP

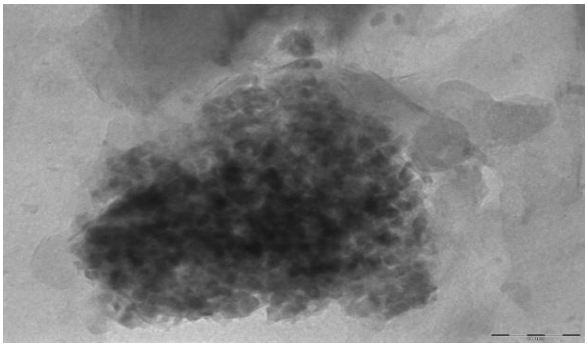

Fig.3. (d) TEM image of TOPO

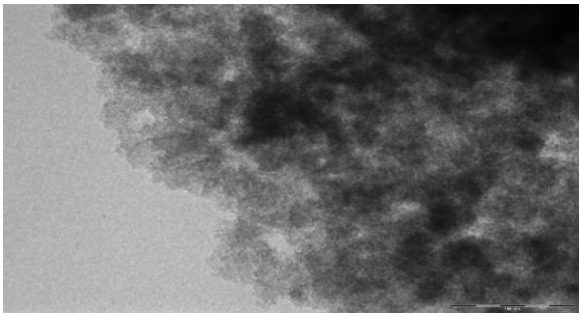

Fig.3. (e) TEM image of the CTAB

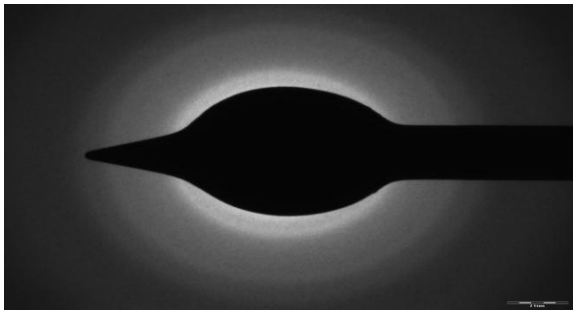

Fig.3. (f) The reprentative selected area diffraction patterns (SAED) of PVP capped ZnS:Mn^{2+} nanoparticles.

This supports, that the size of the synthesized ZnS;Mn^{2+} nanoparticles are in consistent with XRD result. Fig. 3(f) shows the representative selected area diffraction patterns (SAED) of PVP capped ZnS: Mn^{2+} nanoparticles. These are indexed to the (111), (220) and (311) planes which are confirmed the cubic phase. The broad diffuse rings obtained for PVP capped ZnS:Mn^{2+} are due to small crystalline sizes. However, SAED pattern of PVP capped ZnS: Mn^{2+} has more intense diffuse rings which indicates the formation of small crystalline size.

FT-IR spectral studies

Fig. 4(a-d) shows FT-IR spectra of the ZnS 3%, ZnS:Mn^{2+}, PVP, TOPO and CTAB capped ZnS:Mn^{2+} (3%) nanoparticles. From the FT-IR analysis of uncapped ZnS nanoparticles (Fig. 4a) the peaks appearing at 1110, 618 and 491 cm^{1} are due to ZnS vibrations. The obtained peak values are in good agreement with the reported literature. The peaks at 1133 and 1112 cm^{-1}.

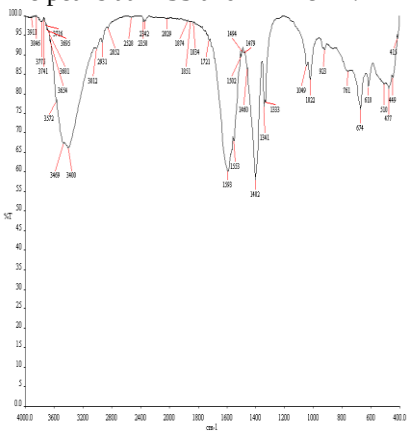

Fig.4. (a)FT- IR spectrum of pure ZnS

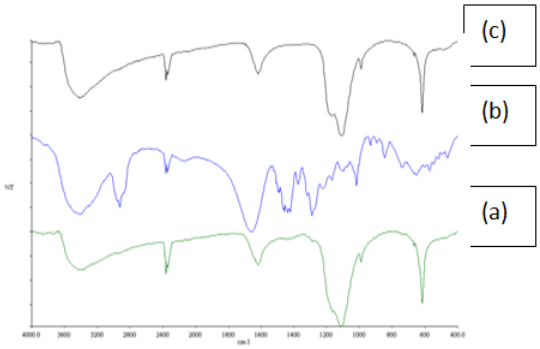

Fig.4. (b) `FT-IR spectra of pure PVP (a) ZnS: 3% nanoparticles (b) pure PVP (c) ZnS:Mn 3% PVP

Fig. 4(b) show the presence of the doping ions (Mn^{2+}) in ZnS. Moreover, the transmittance peaks of the ZnS: $Mn^{2+}$are slightly shifted towards lower wavenumber side from the uncapped ZnS, which may be due to the presence of the doping ions.

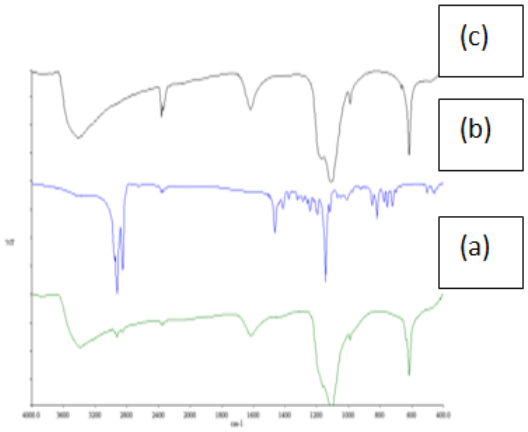

Fig.4. (c) FT-IR spectra pure of TOPO (a) Zn:Mn 3% nanoparticles (b) TOPO (c) ZnS:Mn 3% TOPO

These peaks are slightly shifted to higher wave number side with decrease in intensity when ZnS:Mn^{2+} nanoparticles are capped with surfactants. In the FT-IR spectrum of the composite (Fig. 4c), the transmittance peak around 1700 –1750cm^{-1} are the characteristics of C=O stretching vibration of PVP. In addition, the peak at 1150 cm^{-1}, 1191 cm^{-1}, 1240 cm^{-1} and 1269 cm^{-1} also represent C–O–C stretching vibration of PVP [18]. The spectra for CTAB is presented in Fig.(4a-c).

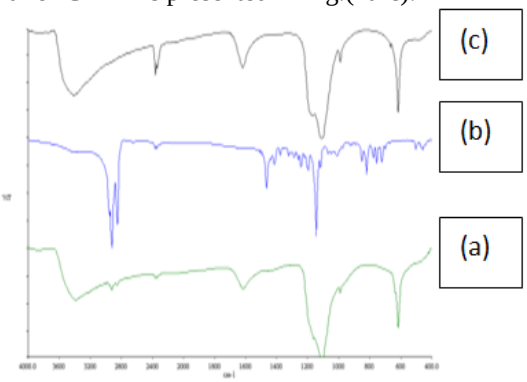

Fig.4(d) FT – IR spectra of pure CTAB (a) ZnS:Cu (nanoparticles),(b) Pure CTAB (c) ZnS:Cu3% CTAB

The strong peaks observed at 1610 and 1402 cm^{-1} are shifted to longer wave number side from the uncapped particles Fig. 4(a-c)), which indicates the presence of CTAB on the ZnS:Mn^{2+} surface. The broad absorption peaks for all the samples in the range of 3410–3465cm^{-1} corresponds to –OH group, which indicate the existence of water absorbed in the surface of nanocrystals. The presence of this band can be clearly attributed to the adsorption of atmosphere water during FT-IR measurements. The peaks at 1500–1650 and 2360–2343 cm^{-1} are due to the C=O stretching mode arising from, the absorption of atmospheric CO_2 on the surface of the nanoparticles [19]. Fig. 4(a–d) shown the FT-IR spectra of ZnS(a) ZnS:Mn^{2+} (b) and surfactants (PVP, TOPO (c) and CTAB (d)) capped ZnS:Mn^{2+} nanoparticles.

UV–visible study

The room-temperature UV–visible absorption spectra of freshly -prepared undoped and Mn^{2+} ions doped ZnS, PVP, TOPO and CTAB capped ZnS: Mn^{2+} nanoparticles (Fig.5) shows the absorption band position in the ultraviolet range. The absorption band of different concentrations of Mn^{2+} doped ZnS nanoparticles has no change in the position (not shown). However, the relative intensity is changed. Among the four different concentrations (1 % – 4 %), the 3% of Mn^{2+} doped ZnS given strong absorption. For this reason, the 3% of Mn^{2+} was selected as an optimum concentration for other studies. In addition, the absorption band of the surfactant capped particles have no change with respect to the capping concentrations (not shown). But the shifting was observed. As observed in Fig.5, the samples exhibit the absorption band at around 315(4 eV), 310(3.94 eV), 302 (4.6 eV), 288 (4.31 eV) and 298(4.16 eV) nm for ZnS, ZnS: Mn^{2+}, PVP, TOPO and CTAB capped ZnS:Mn^{2+} nanoparticles, respectively. The absorption band of all samples were strong by blue shifted as compared with 345 nm (3.6eV) of bulk ZnS.This blue shift of the band gap takes place because of the quantum confinement effect . Has Comparing the three absorption values, the PVP capped ZnS: Mn^{2+} is more blue shifted than the others. It may be due to reduction of the particle size. According to Kumbhojkar et al , the properties of nanocrystalline materials show deviation from the corresponding bulk Properties when the sizes of the crystallites become comparable to the Bohr excitonic radius.

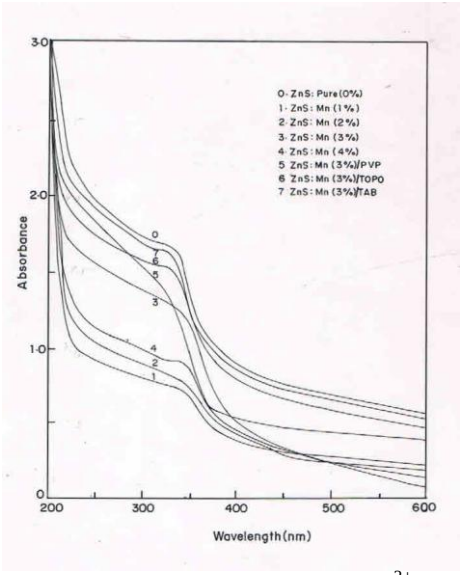

Fig.5. Uv -Vis absorption of ZnS , ZnS : Mn^{2+} (1-4%) and different surfactant (PVP , TOPO and CTAB)

Photoluminescence study

Fig 6(a) shows the room temperature photoluminescence [PL] spectra of the undoped and different concentration (1 % - 4 %) of Mn^{2+} doped ZnS nanoparticles. It can be observed that the PL spectrum of the undoped sample shows a blue emission peak centered at 450 nm which could be ascribed to a recombination of electrons at the sulfur vacancy donor level with holes trapped at the zinc vacancy acceptor level. For the Mn^{2+} doped ZnS nanoparticles, instead of the single peak (ZnS) additional peaks were observed in the blue and green region with enhanced intensity. When Mn^{2+} ions were doped in to the ZnS nanoparticles, more defect states were introduced. Therefore, it is reasonable that the PL intensity is enhanced for the doped samples compared to undoped samples. Fig.6(a) shows that the emission peaks of the Mn^{2+} doped samples exhibits red shift from 450 nm through 460nm, 470 nm, 480 nm and 500 nm for increasing concentration of Mn^{2+} (1 % through 2 %,3 %, and 4 %).The relative intensity also varied significantly. The PL emission observed in this work is quite different from what has been reported in the literature for nano ZnS, Mn^{2+} [22, 24]. Recently murugadoss et.al [24] have reported a red shift of the PL emission with increasing concentration of ZnS, Mn^{2+}. In the present work a red shift was observed that correlated with the increasing concentration of the Mn^{2+} from (1 % - 4 %). The green light position were systematically shifted to longer wave length and moreover the intensity of the ZnS:Mn^{2+} was decreased by higher concentration of the Mn^{2+} ions. This

illustrates an optimum concentration (3 % of doping Mn^{2+} ions for enhanced PL emission). When Mn^{2+} ions were incorporated in ZnS host lattice, the luminescence centre of Mn^{2+} ions are formed. Hence, from the PL emission spectrum, it can be concluded that the Mn^{2+} ions are incorporated successfully in the ZnS host lattice. Fig.6(b) shows the PL spectrum of water soluble PVP, TOPO and CTAB capped ZnS:Mn^{2+} (3 %) nano particles. In the capped particles, the PL intensity is increasing nearly 40-60 compared to the uncapped particles owing to an increase in radioactive recombination efficiency based on passivation of the surfaces from broken surface bonds, adsorbed moisture and oxidizer. Comparison of the PL intensity indicated that the PVP, capped ZnS:Mn^{2+} nanoparticles emission is significantly increased as compared to other surfactant capped particles. This could be a unique characteristic of PVP (which acts as the solvent as well as the capping agent) Moreover, the PVP has a strong dipole movement from nitrogen – oxygen bond, which allows this compound to bind to metal ions. Because the PVP molecules are completely covered on the Zns:Mn^{2+} surface, the surface defect is completely eliminated and the crystallinity is improved. Thus enhanced PL emission was observed. The position of the PVP capped ZnS:Mn^{2+} peak is very sharp and centered at 500 nm and a small peak is observed at 494 nm on ZnS Mn^{2+} that is capped with another effective surfactant TOPO shows an enhanced and narrower PL intensity than the uncapped particles. Comparison of the PL intensities indicates that the TOPO capped ZnS;Mn^{2+} nanoparticles emission significantly increases when compared to other surfactant capped particle. This could be a unique characteristic of TOPO (which acts as good capping agent) moreover the TOPO has strong dipole moment from phosphorus - oxygen which allows the compound to bind to metal ions. The CTAB capped particles gave a peak positioned at 475 nm in the PL emission spectrum.

Further more, the PL enhancement indicates of the PVP capped ZnS:Mn^{2+} intensity is higher than the other surfactant capped particles. Thus it is concluded that the PVP surfactant plays a vital role in the reduction of particle size and also improvement of crystal quality, resulting in a narrow and enhanced PL emission.

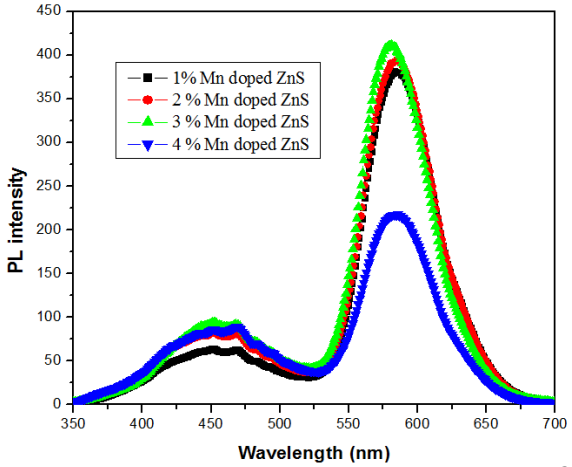

Fig.6. (a) PL spectra of different concentration of Mn^{2+} (1%-4%) doped ZnS nanoparticles.

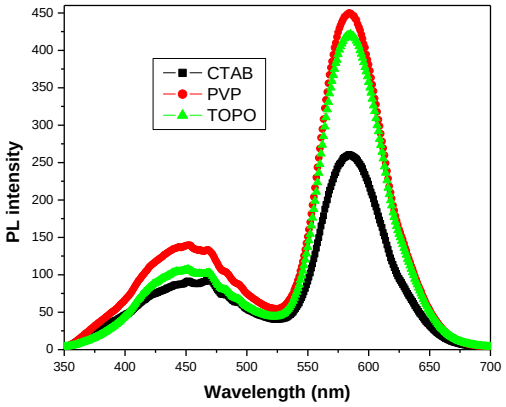

Fig 6 (b) Zns: Mn^{2+} 3% with diffrentent surfactant capped PVP,TOPO and CTAB.

Thermal study

The TG-DTA thermograms were recorded for ZnS:Mn^{2+} (3 %) nanoparticles in the temperature range room temperature (RT) to1000^{0}C with an increase by 10 ºC/min in air atmosphere. Fig.(7) shows combined plots of TG and DTA. From the TGA data plots, it is noticed that the weight loss of the nanoparticles are found to take place up to 700^{0}C. In the first endothermic peak was found at 65^{0}C. This peak are attributed to the evaporation of the water and organics. The exothermic peak around 230^{0}C probably corresponds to the evaporation and lattice deformation of ZnS. The composition does not vary in the nearing range from100^{0}C to 200^{0}C, whereas as can be seen, beyond 230^{0}C, most Mn^{2+} ions are released from the ZnS matrix. The observed endothermic peak at 330^{0}C was believed to be the beginning of phase transition. A broad exothermic peak at 400^{0}C implies the improvement of the crystallinity of the sample. Additionally, above 500^{0}C, there is a smooth downward trend in DTA curve. This may be due to release of residual sulfur ions from the sample.

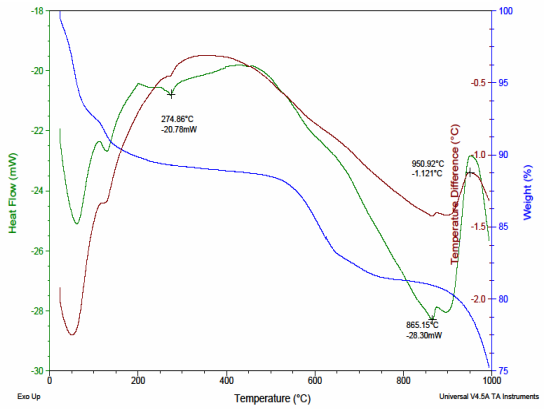

Fig.7. TG-DTA specrta of ZnS : Mn $^{2+}$ nanoparticles ESR STUDY

The local environment of the Mn^{2+} ions in the nanoparticales was probed using ESR. The ESR spectrum of a freshly powdered Mn (3%) – doped ZnS sample showed an intense signal, which could be attributed to Mn - Mn interactions (Fig.8). The six lines which appeared in the ESR spectra were attributed to (ΔMI = 0 and ΔMs =

±1) allowed transitions of the Mn^{2+} ions (I=5/2). These lines were accompanied by smaller ones between them which are assigned to ΔMI = 0 and ΔMs = ±1. The appearance of the well-resolved hyperfine structure together with the less intense lines between them (at approximately g = 6.2) proved that many Mn^{2+} ions were at nearly cubic symmetry. The slight broadening of the ESR spectrum suggested that ex-change coupling may have been occurring in this sample. The spectra also showed a weak, partially resolved hyperfine structure superimposed on a broad background signal (Fig.8). This is characteristic of manganese (II) ions in tetrahedral sites, which could be attributed to manganese incorporated into the ZnS lattice.

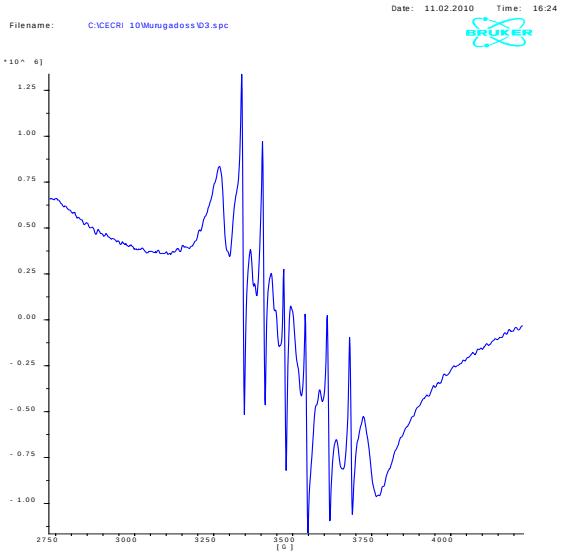

Figure 8 ESR spectrum of (ZnS:Mn^{2+})

IV. Conclusion

Undoped, different concentrations of Mn^{2+} (1 %–4 %)-doped and surfactant-capped ZnS:Mn^{2+} nanoparticles were successfully synthesized by chemical precipitation method in open air using inexpensive equipment. This method may be employed to prepare other monodisperse transition metal-doped semiconductor nano structures that are potentially important for optoelectronic nanodevices. The XRD patterns revealed that the particles exhibited pure cubic crystal structures. The estimated sizes of the uncapped and surfactant-capped nanoparticles were in the range of 1.07-8.5 nm. The absorption spectra of the prepared nanoparticles with different surface modifications (PVP, TOPO and CTAB) and sizes demonstrated the quantum confinement effect. An optimum Mn^{2+} concentration of 3 % was selected based on the results from the PL study. The decreased PL intensity (at higher concentrations of Mn^{2+}) may result from the formation of MnS. The enhanced PL emission of the capped particles shows that the surfactants not only eliminated the surface defects but also improved the crystallinity. Moreover, as the increased PL intensity indicates, the particles grew with a homogeneous size distribution. Furthermore, the samples had good crystal quality and high luminescence sensitivity. Hence, the results suggest the potential applications of the surfactant capped ZnS: Mn^{2+} nanoparticles in optoelectronic devices and nano scale fluorescent probes for biological and medicinal applications.

Table 1: Crystallite size as calculated by using the Debye-Scherrer's formula from XRD table of Full With Half Maximum

Samples	Peak position (111) plane	FWHM	Crystallite Sizes (nm)
Pure ZnS	27.43	0.1673	8.537
1% Mn doped ZnS	27,13	0.1673	8.527
2% Mn doped ZnS	26.84	0.2342	6.089
3% Mn doped ZnS	26.36	0.2676	5.232
4% Mn doped ZnS	28.85	2.7677	5.27
ZnS:Mn 3% (CTAB)	26.95	0.1171	1.218
ZnS:Mn 3% (PVP)	26.73	0.8029	1.072
ZnS:Mn 3% (TOPO)	26.56	0.9368	1.521

Table 2: Band gap of pure and Mn^{2+} ions doped ZnS samples from optical absorption spectrum

Percentage of Mn doped with ZnS	Wavelength (nm)	Energy (eV)
Pure ZnS	340	3.64
1%Mn doped ZnS	340	3.64
2%Mn doped ZnS	345	3.59
3%Mn doped ZnS	350	3.54
4%Mn doped ZnS	360	3.44
ZnS:Mn 3% (CTAB)	360	3.44
ZnS:Mn 3% (PVP)	335	3.70
ZnS:Mn 3% (TOPO)	365	3.39

References

[1] A. Henglein. Ber. Bunsenges. Phys. chem. 86(1982)301
[2] M. Gutierrez. A. Henglein Ber. Bunsenges. Phys. chem.87(1983) 474
[3] A. Henglein. M. Gutierrez. Ch. H. Fischer. Ber. Bunsenges. Phys. chem.87(1983)852
[4] A. Henglein. M. Gutierrez. Ch. H. Fischer. Ber. Bunsenges. Phys. Chem. 88(1984)179
[5] H. Gleites. Progmates. Sci. 33(1989)223
[6] R.W Siegal. Adv Top Mater Sci Erg(1991)273
[7] M. Senna Electrical Phenomena at interfacial surface, surfactant science series. Torohama 1996
[8] H. Schmidt Appl, organomet chem. 15(2001)331
[9] I.Yu. M. Senna, S. Takahashi, Master Res. Bull. 30 [1995] 299.
[10] I.Yu. M. Senna, Appl. Phys. Lett. 66 [1995] 424.
[11] I.Yu. T. Isobe, M. Senna, J. Phys. Chem. Solids 57[1996] 373.
[12] Geng. By. Zhang LD. Wang GZ. Xie T. Zhang YG. Meng GW. Appl Phys Lett 2004:84:2157.
[13] Bhattacharjee B. Ganguli D. Lakoubovesku K. Stremans A. Chaudhuri S. Bull Mater Sci 2002:25:175.
[14] Nanda J. Kuruvilla BA. Sama DD, Phys. Rev. B. 1999:59:7473.
[15] Mach R. muller G. J Cryst Growth 1988:86:866.
[16] Yamaguchi T. Yamamoto Y. Tanaka T. Yoshida A. Thin Solid Films 1999:344:516.
[17] Bredal M. Merikhi J. Mater Sci. 1998:33:471.

[18] Winiarz Jg. Zhang I. Lal. M. Friend CS. Prasad PN, Photogeneration, Charge Transport and photoconductivity of a novel PVK/EdS-nanocrystal polymer composite, Chem Phys. 1999;245:417-28.
[19] Yao JH, Elder KR. Guo H, Grant M. Therory and simulation of Ostwald ripening. Phys. Rev B 1993;47-14110-25.
[20] Qi L, Colfen H, Antonientti M. Synthesis and characterization of Cds nanaoparticles stabilized by double hydrophilic block copolymers. Nano Lett 2001:1:61-5.
[21] Lee YJ, Kim TG, Sung YM. Lattice distortion and luminescence of CdSe/ZnSe nanocrystals. Nanotechnology 2006:17;3539-42.
[22] Dutta J. Hofmann. H. Encyclopedia of nanoscienc and nanotechnology. Americam Scientific Publisher: CA, USA, 2004;617
[23] Murugadoss, G (2010). Synthesis and optical characterization of PVP and SHMP- encapsulated Mn^{2+} doped ZnS nanocrystal. Journal of Liminescence, 130, 2207-2214
[24] Murugadoss, G., Rajamannan, B., & Ramasamy, V. (2010), Synthesis and and opt ical propertiescharacterization of water soluble ZnS;Mn nanoparticles. Journal of Liminescence,130, 2032-2039